Indirect-exchange interactions in disordered metals at finite temperature

Mark R. A. Shegelski* and D. J. W. Geldart
Department of Physics, Dalhousie University, Halifax, Nova Scotia, Canada B3H 3J5
(Received 19 November 1991)

We calculate the effective indirect-exchange interaction between spin-spin pairs in disordered metals. The primary features of this work are that we include intrinsic *sd* exchange scattering and explicitly retain finite temperature in our results. Intrinsic *sd* exchange scattering introduces length scales that strongly affect the structure of the effective interaction. Finite temperature imposes a strictly finite range on the interaction. Finite temperature and *sd* scattering play essential roles in establishing the dependence on impurity concentration of the effective interaction in disordered systems such as metallic spin glasses and dilute ferromagnets.

I. INTRODUCTION

The determination of the effective spin-dependent interaction $H_{\rm eff}(R)$ between localized magnetic moments in a disordered electronic environment is fundamental to the discussion of magnetic properties of many systems. The initial Ruderman-Kittel-Kasuya-Yosida (RKKY) discussion applies to the idealized case of two magnetic moments (spins) in a pure metal in the zero-temperature limit.[1] The characteristic feature of the RKKY indirect exchange interaction is its long-range oscillatory behavior as a function of the distance R between spins, in contrast to the short range expected for direct-exchange interactions. The influence of random disorder in the host environment of these effective spin-spin interactions has been considered by several authors, beginning with de Gennes.[2] One of the central theoretical questions has concerned the extent to which finite electron mean-free-path (λ) effects lead to exponential damping of the spin-spin interactions at large R ($R > \lambda$).

The related experimental questions are to establish how a characteristic magnetic "ordering" temperature depends on the composition of the disordered host (e.g., impurity concentration), and to determine how the details of the range of $H_{\rm eff}(R)$ are reflected in the composition dependence of the ordering temperature. A variety of physical systems have been studied in this context and we will indicate some examples which focus attention on the question of the range of $H_{\rm eff}(R)$. Several types of dilute ferromagnets have been studied. The Curie-Weiss temperatures of a sequence of $(GeTe)_{1-x}(MnTe)_x$ samples, $0 \lesssim x \lesssim 0.5$, have been measured.[3] The dependence of the Curie-Weiss temperature on x in these degenerate semiconductors could be accounted for by the usual damped RKKY interaction in the $x \lesssim 0.15$ composition range but not for $x \gtrsim 0.20$. Dilute magnetic semiconductors such as $Zn_{1-x}Mn_xSe$ have been extensively studied.[4] From data on the spin-glass transition temperatures, it has been concluded that indirect-exchange interactions play an important role in these systems. However, the R dependence deduced for $H_{\rm eff}(R)$ is quite unusual. Dilute metallic spin glasses with concentrations c_i of nonmagnetic impurities have also been investigated.[5] The glass transition temperature $T_g(c_i)$ often exhibits a rapid initial decrease with c_i. This has sometimes been interpreted through the usual damped RKKY interaction, in which $H_{\rm eff}(R) \propto e^{-R/\lambda_i}$ for $R > \lambda_i \propto 1/c_i$. However, it has been argued that the damping factor e^{-R/λ_i} is *not* present in disordered metals at large R ($R > \lambda$) in the low-T limit, and that elastic scattering at large R will have a weak effect on T_g, leaving the decrease in T_g with c_i unexplained.[6-10] Other examples could be given.

The essential conclusions are that the form of $H_{\rm eff}(R)$ in these important classes of disordered systems and the implications for characteristic ordering temperatures are still not well understood. The objective of this work is to present an improved calculation of $H_{\rm eff}(R)$ in disordered systems. The essential features of our work are as follows: (i) A consistent treatment of the intrinsic, spin-dependent scattering of conduction electrons from magnetic ions at finite T introduces length scales in the effective spin-spin interactions. These length scales are inextricably associated with the intrinsic *sd* scattering. (ii) In contrast to the mean free path λ_i due to elastic, pure potential scattering (see above), these length scales *do* appear in $H_{\rm eff}(R)$ in a disordered system and are *essential* for a complete description of the effective interaction. (iii) We explicitly retain finite T in our approach and demonstrate that this is necessary for a complete picture of $H_{\rm eff}(R)$. A brief report of our results has been given previously.[11]

The organization of the remainder of this paper is as follows. In Sec. II, we describe our model and the methods used. The essential Feynman diagrams are summed in Sec. III. Various simplifications are presented in Sec. IV. The bulk of the work is presented in Sec. V, where it is shown that the length scales emerge from the structure of simple poles and branch points in the complex planes of various integral expressions. These results are particularized to low temperature in Sec. VI. We discuss our results and summarize in Sec. VII, focusing on the magnitude and range of the effective interaction.

II. MODEL AND METHODS

In order to calculate a specific form for the effective interaction, we focus on systems consisting of low concentrations of $3d$ magnetic ions and nonmagnetic impurities,

both of which are randomly distributed throughout a metallic host. Examples of such systems include dilute ferromagnets, degenerate semiconductors, and metallic spin glasses, as discussed in Sec. I.

We calculate the effective interaction in the paramagnetic phase where spin-flip *sd* scattering readily occurs. In contrast, spin-flip scattering is less prominent in the low-temperature magnetic phase because the individual spins have preferred directions. Other physical effects differ between the two phases as well. Our objective is to obtain a form for $H_{\rm eff}(R)$ which can be used to describe trends in transition temperatures as a function of impurity concentrations and types. This is most easily accomplished by calculating $H_{\rm eff}$ in the paramagnetic phase and focusing on temperatures close to the transition temperature, as opposed to working in the lower-temperature magnetic phase.

The Hamiltonian which models such systems is $\tilde{H}=H_0+V_{sd}+V_{\rm imp}$, where H_0 describes the conduction electrons in the pure metal, V_{sd} the scattering of electrons due to the *sd* exchange interaction with magnetic ions, and $V_{\rm imp}$ the elastic scattering of electrons by the nonmagnetic impurities. The Hamiltonian H which describes the effective interaction between pairs of magnetic ions is obtained from $\tilde{H}$ in the usual manner of tracing out the electronic degrees of freedom:

$$H=\sum_{(i,j)}H_{ij}=-2\sum_{(i,j)}\sum_{a,b}J_{ij}^{ab}S_i^aS_j^b\ , \tag{2.1}$$

where $\mathbf{S}_i$ is the spin of magnetic moment i at position $\mathbf{R}_i$, the sum is over all pairs (i,j) of spins and all Cartesian components a,b, and $J_{ij}^{ab}=j_{sd}^2\chi_{ij}^{ab}$; $\chi_{ij}^{ab}=\chi^{ab}(\mathbf{R}_i,\mathbf{R}_j)$ is the nonlocal electronic spin susceptibility for a fixed configuration of $3d$ magnetic ions and nonmagnetic impurities, and j_{sd} is the *sd* exchange constant which enters V_{sd}.

Our objective is to obtain information about the magnitude and range of the effective interaction between a typical pair of moments (i,j) with separation $R=|\mathbf{R}_{ij}|$, for a *typical, particular, configuration* of magnetic ions and nonmagnetic impurities, as opposed to simply the *average* interaction. It has been recognized by several previous investigators[6–10] that the typical values of $H_{\rm eff}$ in a disordered system cannot be extracted from $[H_{ij}]_{\rm av}$ and that it is much better to calculate $[H_{ij}^2]_{\rm av}$ in order to obtain the required estimate of $H_{\rm eff}$ for a typical configuration. We follow this general procedure.[7,10] Specifically, we isolate two spins, $\mathbf{S}_i$ at $\mathbf{R}_i$ and $\mathbf{S}_j$ at $\mathbf{R}_j$, and average H_{ij}^2 over all possible configurations of all other $3d$ spins (position and orientation) and of all nonmagnetic ions (positions). We denote this average by $[H_{ij}^2]_{\rm av}\equiv[H^2(R)]_{\rm av}$. The magnitude and range will be extracted from $\{[H^2(R)]_{\rm av}\}^{1/2}$. We will also examine $[H_{ij}]_{\rm av}\equiv[H(R)]_{\rm av}$.

We use the finite-temperature Matsubara method to evaluate these two quantities. The leading contributions[7,10] to $[H(R)]_{\rm av}$ and $[H^2(R)]_{\rm av}$ at large R $(R>\lambda)$ are given by the Feynman diagrams in Fig. 1. The solid circles correspond to the two spins, $\mathbf{S}_i$ at $\mathbf{R}_i$ and $\mathbf{S}_j$ and $\mathbf{R}_j$, the solid lines indicate full single-particle Green's functions, while the shaded sections indicate sums over all "Cooperon-propagator" (or "maximally crossed" or "particle-hole") ladder diagrams, as well as over all "diffusion-propagator" (or "completely uncrossed" or "particle-particle") ladder diagrams.[12] These infinite sums are denoted by ${}^C\Gamma_{\gamma\delta}^{\alpha\beta}$ and ${}^D\Gamma_{\gamma\delta}^{\alpha\beta}$, respectively, where α,β,γ, and δ are electron spin indices.

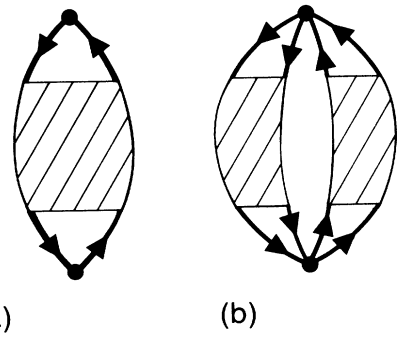

FIG. 1. The Feynman diagrams used to calculate (a) $[H_{ij}]_{\rm av}$ and (b) $[H_{ij}^2]_{\rm av}$. In both cases, the two dots correspond to two spins, $\mathbf{S}_i$ at $\mathbf{R}_i$ and $\mathbf{S}_j$ and $\mathbf{R}_j$, while the heavy lines with arrows represent self-consistent, averaged particle propagators. The shaded sections signify that all diffusion-propagator and all Cooperon-propagator ladder diagrams are summed in both (a) and (b).

The most straightforward method of calculating $[H(R)]_{\rm av}$ and $[H^2(R)]_{\rm av}$ is to first evaluate their momentum-space counterparts and then convert to position space, i.e., calculate the Fourier transform $\xi^{ab}(\mathbf{p})$ of $[\chi^{ab}(\mathbf{R})]_{\rm av}$ directly in momentum space, then obtain $[\chi^{ab}(\mathbf{R})]_{\rm av}$ by Fourier transforming back:

$$[\chi^{ab}(\mathbf{R})]_{\rm av}=\int\frac{d^3p}{(2\pi)^3}\xi^{ab}(\mathbf{p})e^{i\mathbf{p}\cdot\mathbf{R}}\ ,$$

and similarly for $[\chi_{ij}^{ab}\chi_{ij}^{cd}]_{\rm av}$; summing over Cartesian indices then gives $[H(R)]_{\rm av}$ and $[H^2(R)]_{\rm av}$.

III. SUMMATION OF DIAGRAMS

None of the previous approaches has considered *sd* scattering. As a result, the details of our calculations differ somewhat from previous works. Using the ansatz[12]

$${}^C\Gamma_{\gamma\delta}^{\alpha\beta}=A_c\delta_{\alpha\beta}\delta_{\gamma\delta}+B_c\boldsymbol{\sigma}_{\alpha\beta}\cdot\boldsymbol{\sigma}_{\gamma\delta}\ , \tag{3.1}$$

where $\boldsymbol{\sigma}$ is the Pauli spin matrix, we readily solve for A_c and B_c to obtain

$$[\chi^{ab}(R)]_{\rm av}^C=-\delta_{ab}k_BT\sum_{\omega_n}[\Psi_2(\omega_n,\omega_n;R)+\Psi_3(\omega_n,\omega_n;R)] \tag{3.2}$$

for the Cooperon-propagator ladder diagrams, and using a similar ansatz for ${}^D\Gamma$ we find

$$[\chi^{ab}(R)]_{\rm av}^D=-2\delta_{ab}k_BT\sum_{\omega_n}\Phi_2(\omega_n,\omega_n;R) \tag{3.3}$$

for the diffusion-propagator ladder diagrams, where

$$\Psi_n(\omega_1,\omega_2;R)\equiv\int\frac{d^3p}{(2\pi)^3}\frac{C_n\psi^2(\mathbf{p},\omega_1,\omega_2;R)}{1-C_n\phi(\mathbf{p},\omega_1,\omega_2)}e^{i\mathbf{p}\cdot\mathbf{R}}\ , \tag{3.4}$$

$$\Phi_n(\omega_1,\omega_2;R)\equiv\int\frac{d^3p}{(2\pi)^3}\frac{C_n\phi^2(\mathbf{p},\omega_1,\omega_2)}{1-C_n\phi(\mathbf{p},\omega_1,\omega_2)}e^{i\mathbf{p}\cdot\mathbf{R}}\ , \tag{3.5}$$

$$\psi(\mathbf{p},\omega_1,\omega_2;R)\equiv\int\frac{d^3k}{(2\pi)^3}G(\mathbf{k},\omega_1)G(\mathbf{p}-\mathbf{k},\omega_2)e^{-i\mathbf{k}\cdot\mathbf{R}}\ , \tag{3.6}$$

$$\phi(\mathbf{p},\omega_1,\omega_2)\equiv\int\frac{d^3k}{(2\pi)^3}G(\mathbf{k},\omega_1)G(\mathbf{p}-\mathbf{k},\omega_2), \tag{3.7}$$

$G(\mathbf{k},\omega_n)$ is the full single-particle Green's function, $\omega_n=(2n+1)\pi k_BT$ is the Matsubara frequency, and the C_n are defined as follows:

$$\begin{aligned}C_0&=C_i+3C_{sd}\ ,\\ C_1&=C_i+C_{sd}\ ,\\ C_2&=C_i-C_{sd}\ ,\\ C_3&=C_i-3C_{sd}\ ,\end{aligned} \tag{3.8}$$

where C_i and C_{sd} give, respectively, the strength of the nonmagnetic impurity and *sd* scattering. The strengths C_i and C_{sd} are given by $C_i=n_iv_i^2$, $C_{sd}=n_mv_{sd}^2$, where n_i and n_m are, respectively, the number densities of nonmagnetic impurities and magnetic ions, and v_i and v_{sd} are, respectively, measures of the strengths $V_{\rm imp}$ and V_{sd}, both taken to be of short range.

The calculation of $[H^2(R)]_{\rm av}$ proceeds in a similar manner, except that it is more complicated. The diagrams contributing to $[H^2(R)]_{\rm av}$ will be grouped as follows: $[H^2(R)]_{\rm av}^D$ and $[H^2(R)]_{\rm av}^C$ will denote the sums of all diagrams having diffusion-propagator ladders on both sides, and Cooperon-propagator ladders on both sides, respectively, while $[H^2(R)]_{\rm av}^{CD}$ will represent the sum of all diagrams where diffusion-propagator ladders appear on one side and Cooperon-propagator ladders on the other. Evaluating the three terms is straightforward and gives the following expressions:

$$[H^2(R)]_{\rm av}^D=j_{sd}^4(k_BT)^2\sum_{\omega_1,\omega_2}(4[\Phi_2(R)]^2(\mathbf{S}_1\cdot\mathbf{S}_2)^2+\{[\Phi_0(R)]^2-[\Phi_2(R)]^2\}S_1^2S_2^2)\ , \tag{3.9}$$

$$[H^2(R)]_{\rm av}^C=j_{sd}^4(k_BT)^2\sum_{\omega_1,\omega_2}(4[\Phi_1(R)]^2(\mathbf{S}_1\cdot\mathbf{S}_2)^2+\{[\Phi_3(R)]^2-[\Phi_1(R)]^2\}S_1^2S_2^2)\ , \tag{3.10}$$

$$\begin{aligned}[H^2(R)]_{\rm av}^{CD}=j_{sd}^4(2k_BT)^2\sum_{\omega_1,\omega_2}&(\Phi_1(R)[\Psi_0(R)+\Psi_2(R)](\mathbf{S}_1\cdot\mathbf{S}_2)^2+\tfrac{1}{4}\{[I_0(R)+I_2(R)][\Psi_0(R)-\Psi_2(R)]\\ &+[I_3(R)-I_1(R)]\Psi_2(R)\}S_1^2S_2^2)\ ,\end{aligned} \tag{3.11}$$

where $\Psi_n(R)\equiv\Psi_n(\omega_1,\omega_2;R)$ is given by Eq. (3.4), and $\Phi_n(R)\equiv\Phi_n(\omega_1,\omega_2;R)$ by Eq. (3.5).

A general evaluation of $[H(R)]_{\rm av}$ and $[H^2(R)]_{\rm av}$ is highly impractical, but these quantities need to be evaluated only in certain special cases which are of physical interest and which will be fully described below. In these cases of interest, the leading asymptotic behaviors of $[H(R)]_{\rm av}$ and $[H^2(R)]_{\rm av}$ can be obtained.

IV. SIMPLIFICATIONS

The fundamental structure exhibited by the effective spin-spin interaction depends crucially on whether the system is at "low temperature" or "high temperature," the two temperature regimes being separated by a temperature scale T_0 defined as

$$T_0\equiv T_F/(\pi k_F\lambda)\ . \tag{4.1}$$

The temperature T_0 readily emerges in the finite T formalism, as will be shown in Sec. V, and may be interpreted physically as follows. At temperature T, thermal fluctuations induce loss of electronic phase coherence on a length scale $\lambda_T\equiv T_F/(\pi k_FT)$. By "low temperature" we mean $T\ll T_0$ and $\lambda\ll\lambda_T$, while "high temperature" will signify that T/T_0 and λ/λ_T are of order unity or greater. We wish to emphasize that the extreme condition $T\gg T_0$ will usually not be realized in the systems described in this paper. We will use the phrase "high T" to mean that T/T_0 and λ/λ_T are of order unity. We will occasionally consider the $T\gg T_0$ extreme and will refer to this as "extremely high T."

Since we will often speak of a quantity being "of order of or greater than" another quantity, we introduce the symbol O, which means "of the order of." We write "$T>O(T_0)$," for example, to indicate that T is greater than a temperature of the order of T_0.

It is appropriate at this point to give specific examples of physical systems which may be categorized as being at "low T" or at "high T," relative to T_0 as discussed above. In the metallic spin glass $Ag_{0.974}Mn_{0.026}$ studied by Vier and Schultz,[5] the largest value of T_0 occurs for minimal nonmagnetic impurity concentration, and is $T_0\approx100$ K, whereas $T_g\approx10$ K. At maximum nonmagnetic impurity concentration, T_0 can be much higher. For example, in Ag-Mn with Sb impurities, $T_0\approx1000$ K while $T_g\approx7$ K at maximum Sb concentration.[5] This places Ag-Mn in the "low-T" category. In contrast, a dilute ferromagnet having a transition temperature of several hundred K can easily be in the "high-T" category, provided the sample is clean enough that $T_0<O(100\ \text{K})$ (viz., $\lambda\gtrsim100$–200 Å). One example is the Heusler alloy $Cu_2Mn_{0.6}Ni_{0.4}Sn$ for which $\Theta_F\approx350$ K.[13] Alternatively, a ferromagnet with a relatively high degree of disorder (e.g., $\lambda\approx20$ Å) could readily be in the "low-T" regime.

Evaluation of the high-T structure of the effective interaction is readily formulated once the low-T structure has been established. Moreover, the low-temperature

form of the effective interaction for *two* spins in a disordered metal has been studied previously.[7,10] Our focus in this paper will be mostly on the low-T structure of the interaction for the case of a *finite* concentration of spins in a disordered metal. We will discuss the high-T structure only briefly. In forthcoming publications, we will use the low-T form to calculate T_g in metallic spin glasses, and we will provide the details of the high-T form and use the result to calculate T_c in dilute ferromagnets which fall in the high-T regime.

At low T, $[H(R)]_{\rm av}$ gives an extremely misleading picture of the effective interaction, $[H^2(R)]_{\rm av}$ providing a much better estimate.[10] This is because the fluctuations in $H(R_{ij})$, from one particular configuration to another, are enormous compared to the average $[H(R)]_{\rm av}$ over all possible configurations. Consequently, $[H(R)]_{\rm av}$ is a very poor measure of the strength and range of $H_{\rm eff}(R)$. A much improved estimate of the magnitude of $H_{\rm eff}(R)$ is obtained by calculating $[H^2(R)]_{\rm av}$. Therefore, we subsequently concentrate solely on $[H^2(R)]_{\rm av}$.

We next show that, at low T, the integrals $\Psi_n(R)$ in Eq. (3.11) are negligible compared to the $\Phi_n(R)$ in Eqs. (3.9) and (3.10). Consequently, we can neglect $[H^2(R)]_{\rm av}^{CD}$ compared to $[H^2(R)]_{\rm av}^{C}$ and $[H^2(R)]_{\rm av}^{D}$. This leaves

$$[H^2(R)]_{\rm av}=j_{sd}^4 g^2(R)[\,A(R)S_i^2S_j^2+B(R)(\mathbf{S}_i\cdot\mathbf{S}_j)^2\,]\ , \tag{4.2}$$

where

$$g(R)\equiv 2mk_F/(2\pi R)^3\ , \tag{4.3}$$

$$A(R)\equiv I_0(R)-I_1(R)-I_2(R)+I_3(R)\ , \tag{4.4}$$

$$B(R)\equiv 4[I_1(R)+I_2(R)]\ , \tag{4.5}$$

and

$$I_n(R)\equiv g^{-2}(R)(k_BT)^2\sum_{\omega_1,\omega_2}[\Phi_n(\omega_1,\omega_2;R)]^2\ , \tag{4.6}$$

with $n=0$, 1, 2, or 3.

The proof that $\Psi_n(R)$ is negligible begins with the observation that simple poles can exist in the integrands of Eqs. (3.4) and (3.5) and that one of these simple poles could give the dominant contribution to $\Psi_n(R)$ if its imaginary part p_I is small compared to the imaginary parts of other singular points, such as branch points, in the complex p plane. This will indeed be the case for several examples of physical interest. The magnitude of $\Psi_n(R)$ will depend on the magnitude of $\psi(\mathbf{p};R)$ at the simple pole. We show below that these simple poles are close to the origin. Evaluation of $\psi(\mathbf{p};R)$ as $|\mathbf{p}|\to 0$ is straightforward. Comparing the result with a similar evaluation of $\phi(\mathbf{p};R)$ as $|\mathbf{p}|\to 0$ reveals that the integrals $\Psi_n(R)$ are a factor of order $(k_FR)^2$ smaller than the integrals $\Phi_n(R)$. Since $R>\lambda$, $k_FR\gg 1$, and any integral $\Psi_n(R)$ may be neglected compared to a $\Phi_n(R)$ integral. This establishes Eq. (4.2) as a simplification of Eqs. (3.9)–(3.11).

Next, we calculate $\phi(\mathbf{p},\omega_1,\omega_2)$ and use the result to evaluate $\Phi_n(\omega_1,\omega_2;R)$ and, in turn, $I_n(R)$. We calculate ϕ *exactly* by doing the angular integration first, followed by an integration in the complex k plane. Careful treatment of the branch cuts gives

$$\phi(p,\omega_1,\omega_2)=\frac{im^2}{2\pi p}[\mathrm{Ln}(k_1+k_2+p)-\mathrm{Ln}(k_1+k_2-p)]\ , \tag{4.7}$$

where $p=|\mathbf{p}|$ and $\mathrm{Ln}(w)$ is defined by

$$\mathrm{Ln}(w)\equiv \ln r+i\theta,\quad -\pi<\theta\le\pi, \tag{4.8}$$

with $w=re^{i\theta}$, r and θ real; the k_j $(j=1,2)$ are defined in terms of the ω_j by

$$k_j\equiv k_F(1+i\tilde{\omega}_j/\varepsilon_F)^{1/2}\ , \tag{4.9}$$

where $\mathrm{Im}(k_j)>0$ by definition and

$$\tilde{\omega}_j\equiv\omega_j-\mathrm{Im}[\Sigma(\omega_j)]=\omega_j+\mathrm{sgn}(\omega_j)/(2\tau)\ . \tag{4.10}$$

The self-energy $\Sigma(\mathbf{p},\omega_n)$ has been evaluated self-consistently in a Born approximation. The mean free time τ is the total mean free time due to both elastic collisions with the impurities as well as *sd* scattering by the magnetic ions, and is related to C_0 by $\tau=\pi/(mk_FC_0)$.

In view of Eqs. (3.5), (4.6), and (4.7), the values of $\Phi_n(R)$ and $I_n(R)$ will be given in terms of the branch point at k_1+k_2 and/or the simple pole at p_s. If the simple pole exists, it will be given by $1-C_n\phi(p_s,\omega_1,\omega_2)=0$. Our next task will be to investigate the existence and location of these simple poles, to compare their locations to the branch point, and to obtain a suitable approximation for $[H^2(R)]_{\rm av}$.

Before turning to this task, we simplify our expression for $[H^2(R)]_{\rm av}$ one step further. Our ultimate objective is to obtain the magnitude and range of the effective interaction between spin pairs in a disordered metal. We emphasize that, although $[H^2(R)]_{\rm av}$ is, by definition, an averaged quantity, it contains valuable information about the magnitude and range of the effective interaction between pairs of spins *in a particular configuration*.[14] More specifically, we can extract from $[H^2(R)]_{\rm av}$ the magnitude of the effective interaction between an average, typical pair of spins with separation $R=|\mathbf{R}_{ij}|$ in a typical, particular, configuration of nonmagnetic impurities and magnetic ions. To do so, we average Eq. (4.2) over all pairs (i,j) with separation $R=|\mathbf{R}_{ij}|$ in a particular configuration. We denote such an average of $[H^2(R)]_{\rm av}$ by $\langle[H^2(R)]_{\rm av}\rangle$, and we introduce the quantity $K(R)$, defined by

$$\langle[H^2(R)]_{\rm av}\rangle=[K(R)]^2S_i^2S_j^2\ , \tag{4.11}$$

which gives

$$K(R)=j_{sd}^2g(R)[I_0(R)+I_1(R)+I_2(R)+I_3(R)]^{1/2}\ . \tag{4.12}$$

Since $K(R)$ contains the information we seek about the magnitude and range of the spin-spin interaction, we will phrase our discussion in terms of $K(R)$ rather than $[H^2(R)]_{\rm av}$.

V. THE SIMPLE POLES

There are many calculations to be discussed in this section. In order to assist the reader, we begin by presenting a summary of the results. We find a special temperature, T_0, which separates the physical behavior of the system into a "low-temperature" regime ($T \ll T_0$), and a "high-temperature" regime ($T \gtrsim T_0$). At low T, we find simple-pole solutions which allow us to evaluate $I_n(R)$, and hence also $K(R)$, thereby providing us with information about the magnitude and range of effective interactions between spin pairs. We also find that the simple-pole locations depend strongly on the ratio ρ/ρ_{sd}, where ρ_{sd} is the resistivity due solely to the *sd* scattering by the magnetic ions, and ρ is the total resistivity. Although it is highly impractical to calculate $K(R)$ explicitly for all values of ρ/ρ_{sd}, the simple-pole locations and the principal behavior of $K(R)$ are readily obtained asymptotically for "low ρ" (ρ a few times ρ_{sd}, at most) and "high ρ" ($\rho \gg \rho_{sd}$).

Since the route to obtaining these results is unavoidably complicated, it will be helpful to sketch the main steps involved. It will turn out that we will encounter five situations where we will need to consider various "cases" for the quantities involved. We will first distinguish between $I_0(R)$ ($n=0$) and $I_n(R)$ ($n=1,2,3$), since the solutions for $n=1,2,3$ are readily obtained once we have those for $n=0$. The next of these situations will be to separate the pair ω_1,ω_2 into two cases: ω_1 and ω_2 of like sign ($\omega_1\omega_2>0$), and ω_1 and ω_2 of opposite sign ($\omega_1\omega_2<0$). Since no simple poles exist when $\omega_1\omega_2>0$, we will focus on the case $\omega_1\omega_2<0$. In discussing the case $n=0$, we will encounter the quantity $\Delta\omega\tau=(\omega_1-\omega_2)\tau$ (we take $\omega_1>0>\omega_2$), which will lead to the two cases $\Delta\omega\tau \ll 1$ and $\Delta\omega\tau \gg 1$. These cases translate directly into $T \ll T_0$ ("low T") and $T \gg T_0$ ("extremely high T"). The results for the extreme limit $T \gg T_0$ will be used to infer behavior in the $T \gtrsim T_0$ ("high-T") regime. The case $n=1,2,3$ will involve the appearance of quantities α_n. The next two cases to be considered will be $\alpha_n<-1$, for which no simple poles exist, and $\alpha_n>1$. The latter leads to two final cases: $\alpha_n=1+\varepsilon_n$ with $0<\varepsilon_n \ll 1$, which will mean $\rho \gg \rho_{sd}$, and $\alpha_n \gg 1$, which will mean ρ only a few times ρ_{sd}, at most.

For further reference in reading the remainder of this section, we summarize the five sets of cases: (1) $n=0$ vs $n=1,2,3$ [for $I_n(R)$]; (2) $\omega_1\omega_2>0$ vs $\omega_1\omega_2<0$; (3) $\Delta\omega\tau \ll 1$ ($T \ll T_0$) vs $\Delta\omega\tau \gg 1$ ($T \gg T_0$) [for $I_0(R)$]; (4) $\alpha_n<-1$ vs $\alpha_n>1$ (for $n=1,2,3$); and (5) $\alpha_n \gg 1$ ("low ρ," $\rho_{sd}<\rho \lesssim$ a few times ρ_{sd}) vs $\alpha_n=1+\varepsilon_n$, $0<\varepsilon_n \ll 1$ ("high ρ," $\rho \gg \rho_{sd}$).

The existence and location of the simple poles is determined by

$$\mathrm{Ln}(z_b+z)-\mathrm{Ln}(z_b-z)=-2i\alpha_n z \ , \tag{5.1}$$

where

$$z_b \equiv (k_1+k_2)\lambda \equiv x_b+iy_b \ , \tag{5.2}$$

$$z \equiv p_s\lambda \equiv x+iy \ , \tag{5.3}$$

locate the branch point and simple pole, respectively, and

$$\alpha_n \equiv C_0/C_n \ ,$$

with C_0 being the C_n which enters the self-energy and therefore also τ. Since z_b is fixed in terms of ω_1 and ω_2 [see Eqs. (5.2) and (4.9)], it might seem natural to use Eq. (5.1) directly to solve for z in terms of z_b. However, the easiest way to solve for z is to express $[\alpha_n z_b]$ manifestly as a function of $[\alpha_n z]$:

$$[\alpha_n z_b]=-[\alpha_n z]\coth[i\alpha_n z] \ . \tag{5.4}$$

We regard Eq. (5.4) as a relationship which tells us how the location of z_b varies as point z moves about in the complex z plane. Our strategy is to find the value of $[\alpha_n z]$ that gives the value of $[\alpha_n z_b]$ which is fixed by ω_1 and ω_2. We then verify that this value $[\alpha_n z]$ is indeed a solution by using Eq. (5.1). Before considering various cases, note that the definition of $\mathrm{Ln}(w)$, Eq. (4.8), along with Eq. (5.1), restricts $\alpha_n x$ to lie between $\pm\pi$:

$$-\pi<\alpha_n x<\pi \ . \tag{5.5}$$

Also note that, since we will be evaluating Φ_n, Eq. (3.5), only by closing the contour in the upper half-plane, we need consider only $y>0$ and $y_b>0$.

(1) $n=0$, vs $n=1,2,3$

The simplest way to explain our result is to first treat the case $n=0$, $\alpha_n \equiv 1$, describe the solutions found, then extend the results to the cases $n=1,2,3$. We begin by expanding Eq. (5.4) into its real and imaginary parts:

$$x_b=g(x,y)[x(e^{4y}-1)-2ye^{2y}\sin 2x] \ , \tag{5.6}$$

$$y_b=g(x,y)[y(e^{4y}-1)-2xe^{2y}\sin 2x] \ , \tag{5.7}$$

where

$$g(x,y)=[1+e^{4y}-2e^{2y}\cos 2x]^{-1} \ . \tag{5.8}$$

(2) $\omega_1\omega_2>0$ vs $\omega_1\omega_2<0$

Recognizing that $k_B T \ll \varepsilon_F$ and $k_F\lambda \gg 1$, we use Eqs. (5.2), (4.9), and (4.10) to expand z_b in the two cases $\omega_1\omega_2>0$, $\omega_1\omega_2<0$. To be specific, choose $\omega_1>0$, $\omega_2>0$ for one case, $\omega_1>0>\omega_2$ for the other. One easily obtains

$$z_b \sim 2k_F\lambda+i[1+(\omega_1+\omega_2)\tau], \quad \omega_1>0, \ \omega_2>0 \ , \tag{5.9}$$

$$z_b \sim (\omega_1+\omega_2)\tau(1+\Delta\omega\tau)/(2k_F\lambda)+i(1+\Delta\omega\tau), \quad \omega_1>0>\omega_2 \ , \tag{5.10}$$

where $\Delta\omega\tau \equiv (\omega_1-\omega_2)\tau$. (We use the symbol "$\sim$" to signify "is asymptotic to.")

In the case $\omega_1>0$, $\omega_2>0$, Eq. (5.9) indicates that $x_b \sim 2k_F\lambda \gg y_b>1$: the branch point lies just above the real axis and has a large real part. We then see from Eq. (5.1) that the angle between z_b+z and z_b-z, the magnitude of which is $2|x|$ [see Eqs. (4.8) and (5.3)], will be very small unless y is very large (recall the restriction $-\pi<x<\pi$). Equations (5.6) and (5.8) imply that, for $y \gg 1$, x_b is of order one [viz., $x_b=O(1)$], which forces

us to try $y=O(1)$ or $y \ll 1$. Again, Eqs. (5.6) and (5.8) give $x_b=O(1)$ when $y=O(1)$, leaving only the possibility $y \ll 1$, which implies $x \ll 1$ also. That $g(x,y) \gg 1$ for x and y both small raises the possibility of having $x_b \gg 1$, but expanding x_b gives $x_b \sim \frac{2}{3}xy \ll 1$. In summary, when $\omega_1\omega_2>0$, $|x_b| \gg |y_b| > 1$, and there is no way to choose x and y for this to be so: there are no simple poles. We therefore concentrate on the case $\omega_1>0>\omega_2$ [Eq. (5.10)], for which $y_b \sim (1+\Delta\omega\tau) \gg x_b \geq 0$: the branch point lies close to, or on, the imaginary axis.

(3) $\Delta\omega\tau \ll 1$ vs $\Delta\omega\tau \gg 1$

Two separate cases will be examined: $\Delta\omega\tau \ll 1$ and $\Delta\omega\tau \gg 1$, which translate directly into $T \ll T_0$, and $T \gg T_0$, where

$$T_0 \equiv T_F/(\pi k_F \lambda) . \tag{5.11}$$

Note that the minimum value of $\Delta\omega\tau$ is T/T_0. For a metallic spin glass such as Ag-Mn, the values of T_F and λ always give $T_g \ll T_0$, so there are many ω_1,ω_2 pairs satisfying $\Delta\omega\tau \ll 1$, and we are in the "low-T" regime. On the other hand, a dilute ferromagnet could easily have $T_c \gtrsim T_0$, in which case "high-T" behavior will be realized.

When $\Delta\omega\tau \gg 1$, $y_b \sim (1+\Delta\omega\tau) \gg 1$ also. Exploring the dependence of y_b on x and y using Eq. (5.7) quickly leads to the conclusion that $y \gg 1$ when $y_b \gg 1$. Other choices, such as $y \ll 1$, which initially appear to be possible, are easily shown to fail. To leading and next-leading order,

$$x_b \sim x + (2x\cos 2x - 2y \sin 2x)e^{-2y} , \tag{5.12}$$

$$y_b \sim y + (2x \sin 2x + 2y \cos 2x)e^{-2y} , \tag{5.13}$$

from which we obtain

$$x \sim x_b + (2y_b \sin 2x_b - 2x_b \cos 2x_b)e^{-2y_b} , \tag{5.14}$$

$$y \sim y_b - (2y_b \cos 2x_b + 2x_b \sin 2x_b)e^{-2y_b} , \tag{5.15}$$

for the simple pole in the $\Delta\omega\tau \gg 1$ case. Note that the simple pole is exponentially close to the branch point in this case.

When $\Delta\omega\tau \ll 1$, $0 \leq x_b \ll y_b$ and $0 < y_b - 1 \ll 1$. A similar investigation of Eqs. (5.6)–(5.8) leads to the conclusion that $0 \leq x \ll y \ll 1$, for which

$$x_b \sim \tfrac{2}{3}xy, \quad y_b \sim 1 + \tfrac{1}{3}y^2 , \tag{5.16}$$

or

$$x \sim \tfrac{3}{2}x_b[3(y_b-1)]^{-1/2}$$

$$\sim \tfrac{3}{4}(\omega_1+\omega_2)\tau(3\Delta\omega\tau)^{-1/2}(k_F\lambda)^{-1} , \tag{5.17}$$

$$y \sim [3(y_b-1)]^{1/2} \sim [3\Delta\omega\tau]^{1/2} , \tag{5.18}$$

for the simple pole when $\Delta\omega\tau \ll 1$. In this case, the simple pole has a much smaller imaginary part than the branch point.

Next we illustrate an important point. Equations (3.5), (4.7), (5.2), (5.9), and (5.10) show, to leading order, that the branch-point contribution $\Phi^{\rm bp}(\omega_1,\omega_2;R) \propto e^{-R/\lambda}$ for each pair ω_1,ω_2. However, whereas in the case $\Delta\omega\tau \gg 1$ the simple-pole contribution is $\Phi^{\rm sp}(\omega_1,\omega_2;R) \propto e^{-R/\lambda}$ [see Eq. (5.15)], the contribution in the case $\Delta\omega\tau \ll 1$ is

$$\Phi^{\rm sp}(\omega_1,\omega_2;R) \propto e^{-(3\Delta\omega\tau)^{1/2}R/\lambda} \gg e^{-R/\lambda} .$$

The implication is that, at high T, the branch points and simple poles contribute to $I_0(R)$ terms which have the same exponential dependence. On the other hand, the simple-pole contributions dominate the branch-point contributions at low T ($\Delta\omega\tau \ll 1$). Consequently, $I_0(R)$ has markedly different behavior at low T as compared to high T (see below). The exercise of comparing simple-pole and branch-point contributions will be a key procedure when we reach the stage of extracting the dominant contributions to each of the $I_n(R)$ and to $K(R)$.

(4) $\alpha_n < -1$ vs $\alpha_n > 1$

We turn next to locating the simple poles in the case $n=1,2,3$. In extending the simple-pole solutions obtained above to the case $n=1,2,3$, we exploit the feature that $[\alpha_n z_b]$ is precisely the same function of $[\alpha_n z]$ as z_b is of z [see Eq. (5.4)]. From the definition $\alpha_n \equiv C_0/C_n$ and Eqs. (3.8), we have $\alpha_1 = (\eta+3)/(\eta+1)$, $\alpha_2 = (\eta+3)/(\eta-1)$, and $\alpha_3 = (\eta+3)/(\eta-3)$, where $\eta = C_i/C_{sd} > 0$. We may separate the possible values of α_n by noticing that, for any value of $\eta > 0$ and for any choice of n, either $\alpha_n < -1$ or $\alpha_n > 1$.

Consider $\alpha_n < -1$ first. In this case, whether $\omega_1\omega_2 > 0$ or $\omega_1\omega_2 < 0$, there are no simple poles. Running through a series of arguments similar to those used for $n=0$, one can readily show that the requirement $x_b \gg 1$ cannot be satisfied in the case $\omega_1 > 0$, $\omega_2 > 0$, when $\alpha_n < -1$. To treat the case $\omega_1 > 0 > \omega_2$, we make the replacements $z \to \alpha_n z$ and $z_b \to \alpha_n z_b$ in Eqs. (5.6)–(5.8). When $\Delta\omega\tau \gg 1$, the requirement $y_b \gg 1$ [Eq. (5.10)] cannot be satisfied as it was for $n=0$ by having $y \sim y_b$, since the arguments of the exponentials are negative for $y > 0$. Attempting $y_b \gg 1$ via $g(\alpha_n x, \alpha_n y) \gg 1$ leads to $\alpha_n y \to 0^-$ and $\alpha_n x \to 0$: expanding Eqs. (5.6)–(5.8) shows this to be unsuccessful. Similarly, the case $\Delta\omega\tau \ll 1$ also fails to produce a simple pole when $\alpha < -1$.

Simple-pole solutions do exist when $\alpha_n > 1$. The general solution for z can be expressed only implicitly, replacing $z \to \alpha_n z$ and $z_b \to \alpha_n z_b$ in Eqs. (5.6)–(5.8). In principle, these equations could be solved numerically for x and y for each pair ω_1,ω_2 and for a given choice of $\eta = C_i/C_{sd}$. The sums over ω_1,ω_2 in Eqs. (4.2) and (4.6) could then also be evaluated, in principle. The eventual aim of such a calculation could be to obtain $K(R)$ as a function of C_i with C_{sd} fixed. This would be a most ambitious undertaking.

(5) $\alpha_n \gg 1$ vs $\alpha_n = 1+\varepsilon_n$, $0 < \varepsilon_n \ll 1$

Fortunately, we have found a much easier route to obtaining the C_i dependence of $K(R)$. It begins by separating the case $\alpha_n > 1$ into two asymptotic cases: $\alpha_n \gg 1$ and $\alpha_n = 1+\varepsilon_n$, $0 < \varepsilon_n \ll 1$. In each case, forms for x and y, and thus also $K(R)$, are readily obtained. Both cases

are straightforward. The case $\Delta\omega\tau \gg 1$ for $n=0$ gave $y_b \gg 1$ and, in turn, $y \sim y_b$ via Eq. (5.7). Similarly, $\alpha_n \gg 1$ for $n=1,2,3$ gives $[\alpha_n y_b] \sim \alpha_n(1+\Delta\omega\tau) \gg 1$ and, in turn, $[\alpha_n y] \sim [\alpha_n y_b]$. Moreover, replacing $z \to \alpha_n z$ and $z_b \to \alpha_n z_b$, and following the steps used for $n=0$, $\Delta\omega\tau \gg 1$, we easily find

$$x \sim x_b + (2y_b \sin 2\alpha_n x_b - 2x_b \cos 2\alpha_n x_b) e^{-2\alpha_n y_b} , \quad (5.19)$$

$$y \sim y_b - (2y_b \cos 2\alpha_n y_b + 2x_b \sin 2\alpha_n x_b) e^{-2\alpha_n y_b} , \quad (5.20)$$

analogously to Eqs. (5.14) and (5.15). The point is that these results are valid, for $\alpha_n \gg 1$, *whatever the value of* $\Delta\omega\tau$. Thus, *even at low* T ($\Delta\omega\tau \ll 1$), the simple pole is exponentially close to the branch point. The important consequence is that the simple poles associated with the $I_n(R)$ ($n=1,2,3$) do *not* dominate over the branch points, and, as such, $I_n(R) \propto e^{-R/\lambda}$ for $n=1,2,3$. This will be discussed more fully below. It will have major implications for the form of $K(R)$ at low T.

Similarly, the arguments used for $n=0$, $\Delta\omega\tau \ll 1$, wherein we had $0 < x_b \ll y_b = 1^+$, will again apply for the case $\alpha_n = 1+\varepsilon_n$, $0 < \varepsilon_n \ll 1$, $n=1,2,3$. Replacing $z \to \alpha_n z$, $z_b \to \alpha_n z_b = (1+\varepsilon_n) z_b$ gives, for $\Delta\omega\tau \ll 1$,

$$x \sim \tfrac{3}{2} x_b [3(\alpha_n y_b - 1)]^{1/2}$$

$$\sim \tfrac{3}{4}(\omega_1+\omega_2)\tau [3(\varepsilon_n + \Delta\omega\tau)]^{-1/2} (k_F \lambda)^{-1} , \quad (5.21)$$

$$y \sim [3(\alpha_n y_b - 1)]^{1/2} \sim [3(\varepsilon_n + \Delta\omega\tau)]^{1/2} . \quad (5.22)$$

We have retained only the leading terms in ε_n as well as in $\Delta\omega\tau$. The main point here is that the imaginary part of the simple pole is much smaller than that of the branch point, and will therefore dominate when $\alpha_n = 1+\varepsilon_n$, $0 < \varepsilon_n \ll 1$. This will have important consequences for the dependence of $[H^2(R)]_{\rm av}$ on C_i.

Before turning to the final details of calculation of $[H^2(R)]_{\rm av}$, we relate the cases $\alpha_n \gg 1$ and $\alpha_n = 1+\varepsilon_n$ to the overall resistivity ρ, $\rho = \rho_i + \rho_{sd}$. From the expressions given above for α_1, α_2, and α_3, we have

$$\alpha_n = (\rho/\rho_{sd})/[(\rho/\rho_{sd}) - 2n/3] , \quad (5.23)$$

$$\varepsilon_n = 2n/[3(\rho/\rho_{sd}) - 2n] . \quad (5.24)$$

The condition $0 < \varepsilon_n \ll 1$ implies $\rho \gg \rho_{sd}$, while $\alpha_n \gg 1$ requires that ρ/ρ_{sd} exceed $2n/3$ by a small amount. The expressions (5.19) and (5.20) are valid asymptotically for ρ/ρ_{sd} only slightly larger than $2n/3$ but are actually useful even when ρ is a few times ρ_{sd}. This is due to the strong effect of the exponentials in Eqs. (5.6) and (5.7). On the other hand, the asymptotic results of Eqs. (5.21) and (5.22) do not extend quite as far. More specifically, whereas the exponential factors may well pull the $\alpha_n \gg 1$ results as far as $\alpha_n \approx 1$, the considerably weaker power-law behavior for $0 < \varepsilon_n \ll 1$ probably can be pushed no further than about $\varepsilon_n \approx \frac{1}{3}$. These considerations will play a major role when applying our results to obtain the ρ dependence of transition temperatures in various materials.

We turn next to relating the simple-pole locations and branch-point locations to the leading behavior of $K(R)$ as it depends on ρ/ρ_{sd} in the low-T regime.

VI. $K(R)$ AT LOW TEMPERATURE

The principal result of the previous section was to establish under what conditions simple poles exist, and to calculate their locations given those conditions. In this section we will apply these results to obtain the dominant behavior of $K(R)$ at low temperature ($\Delta\omega\tau \ll 1$). We have found that simple poles exist when ω_1 and ω_2 have opposite sign ($\omega_1 > 0 > \omega_2$). The simple poles for $n=0$ at low T are given by Eqs. (5.17) and (5.18). The simple poles at low T for $n=1,2,3$ are given by Eqs. (5.19) and (5.20) at "low ρ" ($\alpha_n \gg 1$), where ρ is a few times ρ_{sd} at most, while the simple poles for "high ρ" ($\alpha_n = 1+\varepsilon_n$, $0 < \varepsilon_n \ll 1$), where $\rho \gg \rho_{sd}$, are given by Eqs. (5.21) and (5.22). We now use these results to evaluate $I_0(R)$ and the $I_n(R)$ ($n=1,2,3$), which will give $[H^2(R)]_{\rm av}$ at low T.

Consider $I_0(R)$ first. Equations (5.9) and (5.10) indicate that the imaginary part y_b of the branch point is of order unity, and is therefore dominated by the simple poles, since $y \sim (3\Delta\omega\tau)^{1/2} \ll 1$; viz., $\Phi_0^{\rm sp} \propto e^{-yR/\lambda} \gg \Phi_0^{\rm bp} \propto e^{-y_b R/\lambda}$. Combining Eqs. (4.6), (3.5), (5.17), and (5.18), and evaluating the simple-pole contribution to $I_0(R)$ gives

$$I_0(R) \sim \left[\frac{3m^2}{4\pi^2 R\lambda}\right]^2 (k_B T)^2 \sum_{\omega_1 > 0 > \omega_2} e^{-2[3(\omega_1-\omega_2)\tau]^{1/2} R/\lambda} \quad (6.1)$$

for the leading behavior of $I_0(R)$ at low T. Further evaluation of the double sum depends on the value of R. If R is not too large, the summation may be well approximated by integration, but if R is large enough, the largest term in the sum will dominate all of the others. These considerations lead to

$$I_0(R) \sim \begin{cases} \frac{3}{16}, & \lambda \lesssim R \lesssim \Lambda_T , \quad (6.2a) \\ \frac{3}{16}(R/\lambda)^2 e^{-2R/\Lambda_T}, & R \gtrsim \Lambda_T , \quad (6.2b) \end{cases}$$

for the leading behaviors of $I_0(R)$ in the two R regimes indicated. Again, the symbol "$\sim$" is used to emphasize the asymptotic nature of these results: we expect Eq. (6.2a), for example, to be a good approximation except when R is quite close to λ or to Λ_T. The well-known length scale Λ_T,

$$\Lambda_T = (\lambda \lambda_T/3)^{1/2} , \quad (6.3)$$

where

$$\lambda_T = T_F/(\pi k_F T) , \quad (6.4)$$

emerges from the condition that the difference between successive values of $[3(\omega_1-\omega_2)\tau]^{1/2} R/\lambda$ be large compared to unity, as discussed above. Just as the length scale λ_T is the finite range of the RKKY interaction between two spins in an *otherwise pure* metal at temperature

$T>0$, Λ_T is the finite range of the indirect exchange interaction between pairs of $3d$ ions in a *disordered* metal at finite temperature T. Whereas the physical origin of λ_T in the former case is simply thermal fluctuations, Λ_T reflects the diffusion-limited propagation of the conduction electrons and is due to combined effects of elastic impurity scattering and thermal fluctuations. We emphasize that $\Lambda_T \ll \lambda_T$ and is certainly finite at any finite temperature and ultimately determines the range of $K(R)$. We will show that Λ_T plays an important role in a complete description of the effective interaction.

A full discussion of the high-T regime will be given elsewhere. However, it is useful to make a short comment at this point. At high T, the simple poles approach the branch points, and $I_0(R) \propto e^{-y_b R/\lambda} \propto e^{-R/\lambda}$. A factor e^{-R/λ_T} also appears at high T. This implies that the effective interaction has a finite range $\Lambda = 1/(1/\lambda + 1/\lambda_T)$ at high T, in marked contrast to the low-T form. Note that Λ will be of order λ if T is of order T_0.

In consequence, the range of the effective interaction between spin pairs depends on whether the physical system falls in the "low-T" category or the "high-T" category. The metallic spin-glass Ag-Mn, for example, has $T_g \ll T_0$, implying a spin-spin interaction range of Λ_T. Alternatively, a dilute ferromagnet with minimal impurities can easily have $\Theta_F > O(T_0)$, giving an interaction range Λ. The role of the finite range in establishing trends in the transition temperatures of various disordered magnetic systems will be discussed elsewhere.

Before presenting the results for $I_n(R)$, $n=1,2,3$, we use Eq. (5.23) to describe the variation of α_n with ρ. If $\rho=\rho_{sd}$ (no nonmagnetic impurities), $\alpha_1=3$, $\alpha_2=-3$, and $\alpha_3=-1$. As ρ increases from ρ_{sd}, α_1 is monotonic decreasing, while $\alpha_2 \to -\infty$ as $\rho/\rho_{sd} \to \frac{4}{3}^-$ and $\alpha_3 \to -\infty$ as $(\rho/\rho_{sd}) \to 2^-$. Moreover, $\rho/\rho_{sd} \to \frac{4}{3}^+$ gives $\alpha_2 \to \infty$, while $\rho/\rho_{sd} \to 2^+$ gives $\alpha_3 \to +\infty$. Finally, α_2 is monotonic decreasing for $\rho/\rho_{sd} > \frac{4}{3}$, while α_3 decreases monotonically for $\rho/\rho_{sd} > 2$. At $\rho/\rho_{sd}=2n$, α_n has decreased to $\frac{3}{2}$. The implication of these considerations is as follows.

When $\alpha_n < -1$, there are no simple poles, so only the branch point contributes to $I_n(R)$. When $\alpha_n \gg 1$, the simple poles are exponentially close to the branch points, so both simple poles and branch points make contributions to $I_n(R)$ in which the same exponential factor appears, viz., $I_n(R) \propto e^{-y_b R/\lambda}$, where $y_b \approx 1$.[15] We have seen in Eq. (6.2a) that $I_0(R) \sim \frac{3}{16}$ for $\lambda \lesssim R \lesssim \Lambda_T$. This will dominate the contributions from $I_n(R)$ $(n=1,2,3)$ for values of ρ small enough that either $\alpha_n < -1$ or $\alpha_n \gg 1$, since these $I_n(R)$ will be exponentially smaller than $I_0(R)$ when $R \gtrsim \lambda$. We are claiming that, for the purposes of comparing $I_n(R)$ and $I_0(R)$, $\alpha_n = \frac{3}{2}$ may be considered to be in the category $\alpha_n \gg 1$. Taken all together, this means we can ignore $I_n(R)$ whenever $\rho_{sd} \lesssim \rho \lesssim 2n\rho_{sd}$, viz., at "low ρ." These considerations give

$$K(R) \sim j_{sd}^2 g(R) [I_0(R)]^{1/2} \tag{6.5}$$

as the leading behavior of $K(R)$ at "low ρ," with $I_0(R)$ given by Eqs. (6.2a) and (6.2b).

As ρ increases further, the α_n decrease until eventually $\varepsilon_n \ll 1$, whereupon we are in the "high-ρ" regime. In this regime, Eqs. (5.21) and (5.22) give the simple-pole locations, which dominate over the branch points, giving

$$I_n(R) \sim \left[\frac{3m^2}{4\pi^2 R\lambda}\right]^2 (k_B T)^2 \times \sum_{\omega_1>0>\omega_2} e^{\{-2[3(\varepsilon_n+\Delta\omega\tau)]^{1/2}\}R/\lambda} . \tag{6.6}$$

As with $I_0(R)$, further evaluation depends on the value of R. For $\varepsilon_n \gg (T/T_0)$, to leading order in ε_n, we obtain

$$I_n(R) \sim \tfrac{3}{16} f_n(R) e^{-2R/\Lambda_n}, \quad \lambda < R < O(\Lambda_n) , \tag{6.7}$$

where

$$f_n(R) = 1 + 2R/\Lambda_n + 4R^2/3\Lambda_n^2 , \tag{6.8}$$

and

$$\Lambda_n = (3\varepsilon_n)^{-1/2}\lambda = \lambda[(\rho/\rho_{sd} - 2n/3)/2n]^{1/2} . \tag{6.9}$$

Before presenting the result for $K(R)$ in the high-ρ regime, some comments are in order. First, we note the appearance of $O(\Lambda_n)$ in Eq. (6.7). The reason for this is mostly easily explained by first combining Eqs. (6.9) and (6.3) to obtain

$$\frac{\Lambda_n}{\Lambda_T} = \left[\left(\frac{3\rho}{2n\rho_{sd}} - 1\right)\frac{\pi k_F \lambda T}{T_F}\right]^{1/2} . \tag{6.10}$$

Consideration of Eq. (6.10) leads to the conclusion that we will never have $\Lambda_n \ll \Lambda_T$ for any of the physical systems of interest. More specifically, in the paramagnetic state with T just above the transition temperature, whether we consider metallic spin glasses or dilute ferromagnets, evaluation of Eq. (6.10) in the low-T, high-ρ regime will always give $0.2 \lesssim (\Lambda_n/\Lambda_T) < 1$. We acknowledge this by using $O(\Lambda_n)$ in Eq. (6.7). The appearance of $O(\Lambda_n)$ in Eq. (6.7) also emphasizes that $f_n(R)$ has important structure which must be considered in its entirety when R is of order Λ_n.

We also emphasize that, for the metallic spin glasses of interest, we will always have $T_g \ll T_0$ (viz., low T). As a result, Λ_n will always be smaller than Λ_T. We have already seen that $\Lambda_n \approx \lambda \ll \Lambda_T$ in the low-ρ regime. Moreover, a straightforward application of Eq. (6.10) readily reveals that $\Lambda_n < \Lambda_T$ in the high-ρ regime, even if $\rho \gg \rho_{sd}$. Consequently, we must take the *sd* length scales Λ_n into consideration. Similar comments apply to disordered ferromagnets which fall in the low-T category.

A simple calculation shows that the opposite extreme $\varepsilon_n \ll (T/T_0)$ is physically unrealizable in the high-ρ regime, and corresponds instead to the ideal limiting case $\rho_{sd}/\rho_i \to 0+$ with all scattering being elastic scattering by nonmagnetic impurities, viz., two spins in a disordered metal. In this ideal case, which has been described by previous workers,[7,10] there are no Feynman diagrams with *sd* scattering, the $I_n(R)$ $(n=1,2,3)$ do not occur, and $K(R)$ is given for all ρ by Eq. (6.5). Equations (6.7)

correspond to the physically realistic case where *sd* scattering must be considered, and we turn next to using Eqs. (6.7) to derive $K(R)$ in the high-ρ regime for *real* systems in which there are finite concentrations of magnetic ions.

Just as Λ_T was the range associated with $I_0(R)$, the Λ_n indicate the ranges of the $I_n(R)$. Combining Eqs. (4.12), (6.2a), and (6.7) gives

$$K(R)\sim j_{sd}^2 g(R)\frac{3^{1/2}}{4}\left[1+\sum_{n=1}^{3} f_n(R)e^{-2R/\Lambda_n}\right]^{1/2}, \quad \lambda \lesssim R \lesssim \Lambda_T , \qquad (6.11)$$

as the leading behavior of $K(R)$ at "high ρ" for $\lambda \lesssim R \lesssim \Lambda_T$; for $R \gtrsim \Lambda_T$, $K(R)$ is exponentially small. For example, physical metallic spin glasses will have $\lambda < \Lambda_n < \Lambda_T$ even if ρ/ρ_{sd} is very large [see Eqs. (6.3) and (6.9)]. As such, we will use Eq. (6.11) for high ρ and Eq. (6.5) for low ρ.

VII. DISCUSSION

The primary result of this paper has been to determine the magnitude and range of the effective interaction between magnetic moments in a disordered metal. The intrinsic roles played by finite temperature, as well as the *sd* scattering due to the 3*d* magnetic moments, have been fully and consistently taken into consideration. The major results are captured in Eqs. (6.5) and (6.11) which give the low-T asymptotic behavior of $K(R)$ in the low-ρ and high-ρ regimes, respectively.

One of the most important features of our work is the appearance of the new length scales Λ_n. These length scales emerge as a consequence of the intrinsic *sd* scattering, and we may therefore denote them collectively by Λ_{sd}. We emphasize, however, that these length scales are due to the combined effects of *sd* scattering (which includes spin-flip scattering) and pure potential scattering (which does not). The combination is revealed via Eqs. (6.9).

The most important consequence of the *sd* scattering is that it leads to a *reduction* in the moment-moment coupling strength at separations of order Λ_{sd}. To understand this reduction, consider first the case of two spins in an otherwise pure metal, for which

$$K(R)=K_0(R)=j_{sd}^2 g(R) . \qquad (7.1)$$

In the "pure metal" case, the factor $g(R)$ implies a $1/R^3$ falloff in the coupling strength as R increases. In the more realistic case of a disordered metal, however, there is a *further* reduction, which goes beyond the $1/R^3$ falloff. This further reduction is revealed by the extra factors in Eqs. (6.5) and (6.11). For example, from Eqs. (6.5) and (6.2a) we see that the interaction strength for moment pairs with $R \gtrsim \lambda$ is a factor $(3^{1/2}/4)$ smaller in the disordered case as compared to the "pure metal" case. If we make the very reasonable assumption that $K(R)\approx K_0(R)$ for $R \lesssim \lambda$, we come to the following conclusion. In the low-ρ regime, where *sd* scattering is dominant, in addition to the $1/R^3$ falloff, the coupling strength between spin-spin pairs drops, as R increases, by a further factor $(3^{1/2}/4)$ at the length scale λ. The length scale λ is actually just Λ_n in disguise; recall the behaviors of the simple poles and the branch points at low ρ. The reduction in coupling strength therefore occurs at the length scale Λ_{sd}, and is due to a combination of *sd* scattering by the magnetic impurities and pure potential scattering by the nonmagnetic impurities. A similar discussion applies at high ρ. In that case, Eq. (6.11) describes a more gradual reduction of $K(R)$ with increasing R, from $K(R)\sim j_{sd}^2 g(R)$, when $R \ll \lambda$, to $K(R)\sim(3^{1/2}/4) j_{sd}^2 g(R)$, when $\lambda \ll R \ll \Lambda_T$. We emphasize that we do not claim a sudden drop by the factor $(3^{1/2}/4)$ at $R=\lambda$ in the low-ρ regime. The Feynman diagrams of Fig. 1 give the leading behavior for $R \gtrsim \lambda$, so that we are restricted to presenting asymptotic results for $R \gtrsim \lambda$. Of course, the reduction in coupling strength at length scale Λ_{sd} occurs not only at low ρ and high ρ, but at intermediate ρ as well.

Another major result of our calculation is that the effective spin-spin interaction has a strictly finite range at all finite T: the coupling goes exponentially to zero for $R \gtrsim \Lambda_T$ at low T, and for $R \gtrsim \Lambda$ at high T.

Note that all the length scales Λ_n and Λ_T, decrease monotonically as ρ increases. The finite range $\Lambda_T \propto \rho^{-1/2}$ for all ρ, whereas the $\Lambda_n \sim \lambda \propto \rho^{-1}$ at low ρ, as compared to $\Lambda_n \propto \rho^{-1/2}$ in the extreme high-ρ regime [viz., $\rho \gg \rho_{sd}$, Eq. (6.9)]. This change in the rate of decrease of Λ_{sd} with increasing ρ will play a major role in affecting the overall behavior of physical transition temperatures: we can imagine shells of radii Λ_T and Λ_{sd} (with $\Lambda_{sd} < \Lambda_T$), centered on a central spin, shrinking as nonmagnetic impurities are added (ρ_i and ρ increasing at fixed ρ_{sd}), and spins with a given R being decoupled from the central spin when ρ increases enough that $\Lambda_T \lesssim R$. Similarly, other spins at R' will suffer a reduction in coupling strength when Λ_{sd} falls below R'. Both processes result in a decrease in the overall spin-spin coupling energy. The overall coupling or "ordering" energy is what drives the spin system toward the ordered state; as the ordering energy decreases so will the ordering temperature. Consequently, the transition temperature will decrease with ρ. The quantitative relation between the transition temperature and ρ, for various physical systems, is planned to be discussed in forthcoming publications.[17]

We also wish to emphasize that Λ_T is the finite range not just on the average, but in *any typical, particular configuration* of nonmagnetic and magnetic impurities. This conclusion follows by recognizing that $[H^2(R)]_{\rm av}$ is exponentially small for $R \gtrsim \Lambda_T$, which implies that the fraction of particular configurations in which $H^2(R_{ij})$ is of order unity when $R_{ij} \gtrsim \Lambda_T$ must also be exponentially small. The important consequence is that the structure of $K(R)$ contains crucial information about the effective spin-spin interaction in a typical, particular configuration.

Finally, we emphasize that the essential physical reason for the strong damping effect of the *sd* scattering is the breaking of time-reversal symmetry by the local magnetic moments of the magnetic ions. Any other interactions which break time-reversal symmetry would

also contribute to this intrinsic self-damping. Extrinsic contributions to the damping of the spin-spin interactions are given by the addition of impurity atoms with spin-dependent interactions, as in the case of spin-orbit scattering.[7,10,16]

Before summarizing, we briefly compare our results with those of previous workers.[6–10,16] We are in agreement that $[H_{ij}]_{\rm av}$ is not an appropriate measure of the strength or range of the indirect exchange interaction, that $[H_{ij}^2]_{\rm av}$ is a better measure, that λ is not the range of the interaction, and that $[H_{ij}^2]_{\rm av} \propto R^{-6}$ for $\lambda < R < \Lambda_T$. Our work reveals the extreme importance of intrinsic *sd* scattering and emphasizes that finite temperature also plays an essential role. One of our principal results is that the magnitude $K(R)$ of the interaction exhibits a decrease at the length scale Λ_{sd}. Similar results have been reported previously in the case of spin-orbit scattering. For example, it has been shown[7] that the interaction strength decreases at the spin-orbit length $\Lambda_{\rm SO}$, provided $\lambda \ll \Lambda_{\rm SO} \ll \Lambda_T$. However, in the case of *sd* scattering at finite T, we have seen that it is not possible to have $\lambda \ll \Lambda_{sd} \ll \Lambda_T$ in the physical systems of interest. The important consequence is that finite T *must* be explicitly retained in the case of *sd* scattering. This is in contrast to previous works[7,10,16] which investigated spin-orbit scattering and considered the case $\lambda \ll \Lambda_{\rm SO} \ll \Lambda_T$; finite T was not required to be explicitly retained in those cases. Other comparisons are possible.

In summary, we have calculated the effective indirect exchange interaction between spin-spin pairs in disordered systems at finite temperature T. We have taken into consideration not only the elastic scattering of electrons by nonmagnetic impurities, but also the intrinsic *sd* exchange scattering by the magnetic ions themselves. The *sd* scattering introduces length scales which give the separations of spin-spin pairs at which the strength of the effective interaction suffers a marked reduction, and which play a major role in establishing the structure of the effective interaction. We emphasize that these length scales are inextricably associated with the intrinsic *sd* scattering. This structure of the effective interaction is revealed in Eqs. (6.5) and (6.11), which give the magnitude $K(R)$ of the effective interaction between a spin pair with separation R. We have also emphasized that the interaction has a strictly finite range at any finite temperature, and that the finite range will play a major role in applications to physical systems of interest.

ACKNOWLEDGMENTS

One of us (M.R.A.S.) thanks several colleagues for stimulating discussions, especially D. Maclean, P. Mulhern, M. Rasolt, V. Srinivas, and D. Zimmerman. One of us (D.J.W.G.) thanks the Gordon Godfrey bequest at the University of New South Wales for support. This work was supported by the Natural Sciences and Engineering Research Council of Canada.

*Present address: Department of Physics, The University of Lethbridge, Lethbridge, Alberta, Canada T1K 3M4.

[1]M. A. Ruderman and C. Kittel, Phys. Rev. **96**, 99 (1954); T. Kasuya, Prog. Theor. Phys. **16**, 45 (1956); K. Yosida, Phys. Rev. **106**, 893 (1957).

[2]P. G. de Gennes, J. Phys. Radium **23**, 630 (1962).

[3]R. W. Cochrane, M. Plischke, and J. O. Ström-Olsen, Phys. Rev. B **9**, 3013 (1974).

[4]A. Twardowski, H. J. M. Swagten, W. J. M. de Jonge, and M. Demianiuk, Phys. Rev. B **36**, 7013 (1987).

[5]See, for example, D. C. Vier and S. Schultz, Phys. Rev. Lett. **54**, 150 (1985).

[6]P. F. de Chatel, J. Magn. Magn. Mater. **23**, 28 (1981).

[7]A. Yu. Zyuzin and B. Z. Spivak, Pis'ma Zh. Eksp. Teor. Fiz. **43**, 185 (1986); [JETP Lett. **43**, 234 (1986)].

[8]L. N. Bulaevskii and S. V. Panyukov, Pis'ma Zh. Eksp. Teor. Fiz. **43**, 190 (1986); [JETP Lett. **43**, 240 (1986)].

[9]G. Bergmann, Phys. Rev. B **36**, 2469 (1987).

[10]A. Jagannathan, E. Abrahams, and M. Stephen, Phys. Rev. B **37**, 436 (1988).

[11]M. R. A. Shegelski and D. J. W. Geldart, Solid State Commun. **79**, 769 (1991).

[12]See A. Kawabata, Prog. Theor. Phys. Suppl. **84**, 16 (1985); P. A. Lee, J. Non-Cryst. Solids **35&36**, 21 (1980).

[13]E. Uhl and R. Sobczak, Solid State Commun. **39**, 655 (1981).

[14]The importance of distinguishing between the average value of a quantity such as $[H(R)]_{\rm av}$ and its value in a particular configuration has been clearly discussed in Ref. 10.

[15]Recognizing that (i) α_2 and α_3 jump from $-\infty$ to $+\infty$ as ρ/ρ_{sd} passes $\frac{4}{3}$ and 2, respectively, and (ii) simple poles do not exist for $\alpha_n < -1$ but do for $\alpha_n > 1$, prompts the question: What contribution do the simple poles make in the limit $\alpha_n \to +\infty$? A straightforward calculation provides the conceptually satisfying result of vanishing contribution as $\alpha_n \to +\infty$.

[16]M. J. Stephen and E. Abrahams, Solid State Commun. **65**, 1423 (1988).

[17]A full investigation of the dependence of T_g on ρ in metallic spin glasses has been reported in M. R. A. Shegelski and D. J. W. Geldart, Phys. Rev. B **46**, 2853 (1992).